Detectability of cold streams into high-z galaxies by absorption lines

Tobias Goerdt
Departamento de Física Teórica, Universidad Autónoma de Madrid, 28049 Madrid, España

Cold gas streaming along the dark-matter filaments of the cosmic web is predicted to be the major source of fuel for disc buildup, violent disk instability and star formation in massive galaxies at high redshift. I investigate to what extent such cold gas is detectable in the extended circum-galactic environment of galaxies via selected low ionisation metal absorption lines. I model the expected absorption signatures using high resolution zoom-in AMR cosmological simulations. In the postprocessing, I distinguish between self-shielded gas and unshielded gas. In the self-shielded gas, which is optically thick to Lyman continuum radiation, I assume pure collisional ionisation for species with an ionisation potential greater than 13.6 eV. In the optically thin, unshielded gas these species are also photoionised by the metagalactic radiation. I compute the absorption line profiles of radiation emitted by the galaxy at the centre of the same halo. I predict the strength of the absorption signal for individual galaxies without stacking. I find that the absorption profiles produced by the streams are consistent with observations of absorption and emission profiles in high redshift galaxies. Due to the low metallicities in the streams, and their low covering factors, the metal absorption features are weak and difficult to detect.

1 Introduction

Cold gas is thought to flow into massive haloes $\sim 10^{12}$ $M_\bullet$ at $z = 2-3$ along filaments with velocities of $\gtrsim 200\,\mathrm{km\,s^{-1}}$. This phenomenon is predicted by simulations and theoretical analysis, where high-z massive galaxies are continuously fed by narrow, cold, intense, partly clumpy, gaseous streams that penetrate through the shock-heated halo gas into the inner galaxy[?]. Indeed, hydrodynamical cosmological simulations reveal that the rather smooth gas components, including mini-minor mergers with mass ratio smaller than 1:10, brings in about two thirds of the mass[?]. But it seems that only a small fraction of the LBGs exhibit redshifted absorption features, which was interpreted as an indication for the absence of cold streams in haloes with $4\times10^{11} < M_\mathrm{v} < 10^{12} M_\bullet$[?][hereafter S10]. The goal of this study[?] is to predict the absorption-line signatures of the cold flows, for a detailed comparison with observations like S10.

[?] used cosmological hydrodynamical AMR simulations to predict the characteristics of Lyα emission from the cold gas streams. The Lyα luminosity in their simulations is powered by the release of gravitational energy as the gas is flowing with a rather constant velocity down the potential gradient toward the halo centre. The simulated Lyα-blobs (LABs) are similar in many ways to the observed LABs. Some of the observed LABs may thus be regarded as direct detections of the cold streams that drove galaxy evolution at high z. Observations seem to support this picture[?].

2 The Simulations

We use three simulated galaxies from a suite of simulations, employing Eulerian adaptive mesh refinement (AMR) hydrodynamics in a cosmological setting. These are zoom-in simulations in dark-matter haloes with masses $\sim 5 \times 10^{11}$ $M_{\odot}$ at $z = 2.3$, with a maximum resolution of 35 - 70 pc in physical coordinates [?](hereafter CDB).

3 Computing the ionisation states

In order to compute the ionisation states via post-processing we take the densities, temperatures and metallicities from the simulation. We assume a primordial helium mass fraction $Y = 0.24$, corresponding to a helium particle abundance of 1/12 relative to hydrogen. For the heavy elements we assume the [?] solar photosphere pattern.

We determine whether a given simulation cell is "self-shielded", i.e. optically thick to Lyman continuum radiation, via a simple density criterion. Cells with total hydrogen exceeding $n_{\rm shield} \equiv 0.01$ cm^{-3} are assumed to be self-shielded. For lower densities the cells are assumed to be optically thin. We calculate the atomic and ionic fractions $x_{\rm Ai}$ using CLOUDY [?], where $x_{\rm Ai}$ is defined as the fractions of element A in ionisation state i.

4 Central source

In this section we consider the Lyα and metal line absorption that occurs as UV light emitted by the central galaxy is absorbed by gas in the circum-galactic environment. As defined by S10, the circumgalactic medium is situated in the spherical zone from just outside the galactic disk to around the virial radius $R_{\rm v}$. Observations of absorption against the central galaxy itself have the advantage of being able to discriminate between inflows and outflows because the absorptions may be assumed to occur in foreground material only. Radiation emitted or scattered from behind the galaxy is blocked by the galaxy itself. However, such absorptions do not provide spatial information about the distance from the galaxy centre as they are all by definition at an impact parameter $b = 0$ from the galaxy centre. S10 employed this technique of observing absorptions against the central galaxy by stacking a sample of 89 galaxies with $z = 2.3 \pm 0.3$ using both rest-frame far-UV and Hα spectra, to investigate the kinematics of the gas flows in the circumgalactic regions.

Along a given sight-line the gas has a varying density, temperature and radial velocity as function of radial position r from the central galaxy. The convolutions of the different densities and radial velocities in the gas along the line of sight are the main ingredients to compute an absorption line profile. This is done as follows: the radial velocity offset Δw relative to central source at rest of all the gas is measured. We assume Voigt profiles with a thermal Doppler broadening parameter

$$b = \sqrt{\frac{2\,k\,T}{m_{\rm A}}}, \tag{1}$$

where k is the Boltzmann constant, T is the temperature of the gas and $m_{\rm A}$ is the mass of the element A. So for angular position (ϕ, θ) we can compute the optical depth $\tau_\nu(\phi, \theta, \Delta w)$ at the velocity offset Δw as

$$\tau_\nu(\phi, \theta, \Delta w) = \frac{\sqrt{\pi}\ e^2\ f_\lambda\ \lambda_0}{m_{\rm e}\ c} \int_{r_{\rm i}}^{R_{\rm v}} \frac{n_{\rm A}(\vec{r})\ x_{\rm Ai}(\vec{r})}{b(\vec{r})}\ H\left[\frac{\gamma_\lambda\ \lambda_0}{4\,\pi\ b(\vec{r})}, \frac{\Delta w - v(\vec{r})}{b(\vec{r})}\right]\ dr, \tag{2}$$

where e is the electron charge, $m_{\rm e}$ is the electron mass, c is the speed of light, λ_0 is the transition wavelength, $n_{\rm A}(\vec{r})$ is the gas density of element A at position $\vec{r} = (\phi, \theta, r)$, x_{Ai} is the ionisation

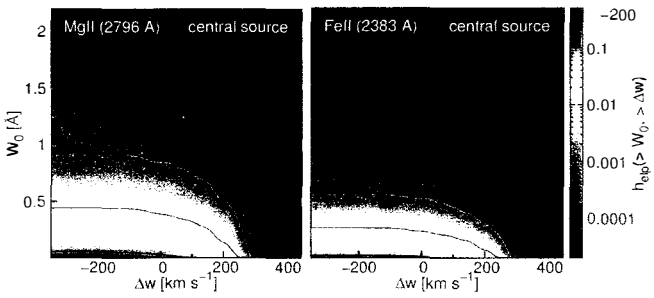

Figure 1: Fraction $h_{\rm elp}$ of all possible example line profiles in the central geometry whose EW is higher than W_0 and whose line centre is at a velocity offset indicating an inflow at least as fast as Δw. Here for the metal lines. Positive velocities are inflowing into the galaxy and negative velocities are out of the galaxy. Contour lines are at 0.1, 0.01, 0.001 and 0.0001 respectively. Note the different y-axis scalings from row to row. In C II one sees an inflow $> 150\,{\rm km\,s^{-1}}$ with an EW > 0.17 Å in 0.4 % of all observations. For Mg II one sees an inflow $> 150\,{\rm km\,s^{-1}}$ with an EW > 0.2 Å in 1.3 % of all observations. The line which has by far the strongest signal is the Mg II line followed by the Fe II line. These values should be achievable by future observations.

fraction of element A in state i, v is the velocity of the gas, f_λ is the oscillator strength of the absorption line and γ_λ is the sum over the spontaneous emission coefficients or the damping width. The Voigt profile is

$$H(a,u) = \frac{a}{\pi}\int_{-\infty}^{\infty}\frac{\exp(-y^2)}{(u-y)^2+a^2}\,dy, \tag{3}$$

where a is the ratio of the damping width to the Doppler width and u is the offset from line centre in units of Doppler widths. Knowing $\tau_\nu(\Delta w)$ it is now possible to compute an absorption line profile $I(\Delta w)$ for a given direction which is simply the function

$$I(\Delta w) = \exp[-\tau_\nu(\Delta w)]. \tag{4}$$

For a fair comparison to the observations done by S10, we mimic a Gaussian point spread function. It has a beam-size (= FWHM η of the Gaussian) of 4 kpc. It is done by splitting up a cylinder with a radius of three times the beam-size into as many parallel fibres as the resolution permits, determining the absorption line profile for every individual fibre and then computing a Gaussian weighted average absorption line profile from all fibres.

Figure ?? is intended to give the likelihood of a detection of a cold stream while looking at a single galaxy from a single direction without averaging. It shows the fraction $h_{\rm elp}$ of all possible example line profiles in the central geometry whose EW is higher than W_0 and whose line centre is at a velocity offset indicating an inflow at least as fast as Δw. The example line profiles are integrated from $1.0\,R_{\rm v}$ down to $0.3\,R_{\rm v}$. Positive velocities are inflowing into the galaxy and negative velocities are out of the galaxy. For Mg II one sees an inflow $> 150\,{\rm km\,s^{-1}}$ with an EW > 0.2 Å in 1.3 % of all observations. These values should be achievable by future observations.

We produce stacked spectra using our simulations by summing up the line profiles of several thousand different directions for each of the three galaxies and stack them together. We determine the absorption line profile for a spherical shell between an outer radius and an inner radius $r_{\rm i}$. The outer radius is always kept constant at 1.0 $R_{\rm v}$ which corresponds roughly to 74kpc. The inner radius $r_{\rm i}$ however is varied between 0.3 $R_{\rm v}$ and 0.02 $R_{\rm v}$. In figure ?? the resulting profiles are shown for all the metal lines. The predicted metal line absorption profiles appear tiny compared to the corresponding lines presented in figures 6 or 10 of S10 having a line depth of 0.5 and $\eta \sim 1000$ km s^{-1} in metals. Probably the most suitable lines for the purpose

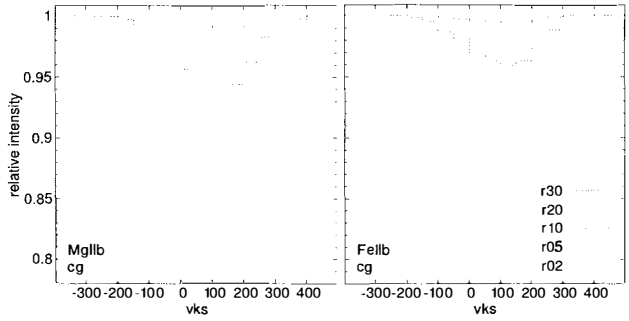

Figure 2: Metal line bsorption profiles for a central source geometry averaged over different viewing angles and all three galaxies. We integrated from 1.0 R_v down to different inner radii r_i. Positive velocities are inflowing into the galaxy and negative velocities are out of the galaxy. Note the different y-axis scaling from row to row. The metal lines are much weaker than the Lyα line, since the inflowing material is mainly unprocessed primordial gas with very low metallicity. These metal lines also appear tiny compared to the corresponding lines presented by S10. The profiles always peak in the positive, indicating inflow.

of detecting cold streams in absorption are C II and Mg II since they have the strongest signal. Out of those Mg II is closer to being observed with the needed sensitivity and resolution.

5 Conclusions

Here we addressed the expected absorption signature from these cold streams. We "observed" simulated galaxies for metal lines from low and medium ionisation ions. We focused on the absorption line profiles as observed by S10, using their set of ten different lines and mimicking their way of stacking data from several galaxies, for sources that are either in the background or at the centre of the absorbing halo itself. The simulations used are zoom-in cosmological simulations with a maximum resolution of 35-70 pc [?]. Self-shielding was accounted for by a simple density criterion.

We conclude that the signatures of cold inflows are subtle, and when stacked are overwhelmed by the outflow signatures. Our predicted Lyα line absorption profiles agree with the observations, while the stacked metal line absorption from the inflows is much weaker than observed in the outflows. The single-galaxy line profiles predicted here will serve to compare to single-galaxy observations.

References

1. Dekel A, Birnboin Y, Engel G. et al, 2009, Nature, 457, 451
2. Steidel C. C, Erb D. K, Shapley A. E, Pettini M, Reddy N. A, Bogosavljević M, Rudie G. C, Rakic O, 2010, ApJ, 717, 289, S10
3. Goerdt T, Dekel A, Sternberg A, Gnat O, Ceverino D, 2012, arXiv:1205.2021
4. Goerdt T, Dekel A, Sternberg A, Ceverino D, Teyssier R, Primack J. R, 2010, MNRAS, 407, 613
5. Erb D. K, Bogosavljević M, Steidel C. C, 2011, ApJ, 740L, 31
6. Ceverino D, Dekel A, Bournaud F, 2010, MNRAS, 404, 2151, CDB
7. Asplund M, Grevesse N, Sauval A. J, Scott P, 2009, ARA&A, 47, 481
8. Ferland G. J, Korista K. T, Verner D. A, Ferguson J. W, Kingdon J. B, Verner E. M, 1998, PASP, 110, 761